



香港天文台
HONG KONG OBSERVATORY

Reprint 900

LIDAR and Chaotic Oscillatory-based Neural Network for
Wind Shear Forecasting

K.M. Kwong*, James N.K. Liu* & P.W. Chan

The 2010 World Congress in Computer Science,
Computer Engineering and Applied Computing
12 - 15 July 2010, Las Vegas, NV, USA

*Hong Kong Polytechnic University, Hung Hom, Kowloon, Hong Kong, China

LIDAR and Chaotic Oscillatory-based Neural Network for Wind Shear Forecasting

K.M. Kwong, James N.K. Liu and P.W. Chan

Abstract— Wind shear, which refers to sudden and sustained changes in the wind direction and speed, could be hazardous to aviation. Windshear is rather difficult to predict due to its transient and sporadic nature. Moreover, the causes of wind shear may be different at different airports. In some places it is caused by microbursts, while in other places wind shear may result from meso-scale weather phenomena and terrain effect. Thus, algorithms and techniques used to predict wind shear caused by microbursts, as in [1], may not be applicable at another airport where wind shear and turbulence arise from other meteorological conditions. This paper focuses on the use of chaotic oscillatory-based neural networks (CONN) for predicting wind shear arising from meso-scale weather phenomenon at the Hong Kong International Airport. Using historical weather data from the Hong Kong Observatory, simulations show that CONN is able to forecast wind shear with a reasonable level of accuracy for a sea breeze event.

I. INTRODUCTION

The term “wind shear” refers to a change in the wind direction and speed that typically lasts 3 to 40 seconds and results in a sustained change in the headwind experienced by aircraft. A decrease in headwind will result in decreased lift and this in turn may mean that an aircraft deviates from its planned flight path [2].

While wind shear may be hazardous to the aircraft, it is also a complex and hard-to-predict phenomenon. One particular difficulty is that the causes of wind shear may be different in different locations. In some places wind shear is caused by microbursts, which are localized columns of sinking air, while in other places wind shear may result from other meso-scale weather phenomena associated with seasonal prevailing winds and local topographies. Thus, algorithms and techniques used to predict wind shear caused by microbursts, as in [1], may not be applicable at other airports such as Hong Kong International Airport (or HKIA), where the main causes of wind shear and turbulence are strong winds blowing across the local hills [3, 4], the winds associated with tropical cyclones, and sea breeze [2]. Wind

Manuscript received January 6, 2010. This work was supported in part by CERG grant B-Q05Z, and LIDAR data kindly provided by Hong Kong Observatory.

K. M. Kwong and James N.K. Liu are with the Hong Kong Polytechnic University, Hung Hom, Kowloon, Hong Kong. (e-mail: cskmkwong@comp.polyu.edu.hk, csnkliu@inet.polyu.edu.hk).

P. W. Chan is with the Hong Kong Observatory, Hong Kong (e-mail: pwchan@hko.gov.hk).

shear is not uncommon at HKIA, where it is experienced by about one in 500 arriving and departing flights with many occurrences being in non-rainy and clear-air conditions [2].

A further difficulty in the prediction of wind shear is that it is difficult to model, not least because it arises over very short time periods. Artificial Neural Networks (ANNs) have been applied with some success to other wind prediction problems. Bilgili, Sahin and Yasar [5] used hourly mean wind speeds and ANNs to predict mean monthly wind speeds. More and Deo [6] used ANNs and wind forecasts to predict the power output of wind turbines. Oztopal [7] used ANNs in predicting the wind potential of various regions. Barbounis et al. [8] used ANNs to forecast long-term wind speeds and their potential for use in generating wind power. In all of these cases, however, the predictions were only of mean hourly or monthly wind velocities covering relatively large regions, making them inapplicable to the very short time frame and localized area of the occurrence of wind shear in the airport region.

One way to deal with the short-term nature of wind shear prediction is to apply chaotic neural networks [9], [10] which model the non-linear behavior of neurons, activating a neuron with a non-linear output function, thereby providing far much more complex behavior than the simple threshold functions used in conventional ANNs. Inclusion of chaotic behavior in ANNs offers the possibility of weather forecasting [11]. Neural network architectures and learning algorithms involving chaos have been used for the storage in memory of analog patterns [12]. While it is hard to apply chaos theory to long-term prediction, it seems that, owing to its ability to focus on the simple deterministic relationship for what would appear to be random-looking data, it may be well-suited to short-term prediction, especially when a good physical model is lacking [13].

In this paper, we propose a meso-scale wind shear prediction model that uses chaotic oscillatory-based neural networks (CONN) to forecast the evolution of winds along the glide path of the airport. The model makes use of accurate Doppler velocities measured using LIDAR (Light Detection And Ranging) data collected by the Hong Kong Observatory at HKIA. LIDAR is an optical analogue of RADAR (Radio Detection and Ranging). It uses a ground-based pulsed laser beam to measure the velocity of aerosols in the air. LIDAR has previously been used to detect occurrences of wind shear, with high accuracy [14], but there has been little research into using it to forecast wind shear. The proposed model is tested in simulations and its predictions were compared with

historical LIDAR data. The model is demonstrated to have the potential of forecasting the time, location and size of wind shear events with considerable accuracy.

The remainder of this paper is organized as follows. Section II describes chaotic oscillators, which form the basis of our chaotic oscillatory-based neural networks (CONN) approach. Section III presents our methodology for applying CONN on wind shear forecasting. Section IV presents our simulation and its results. Section V presents our conclusion and an outline of future work.

II. THE CHAOTIC OSCILLATOR

Wilson and Cowan [15] proposed the neural oscillatory model, which describes the behavior of neurons as interactive triggering between excitatory and inhibitory neurons. This theory has also formed the basis of many subsequent studies and models in cognitive information processing [16] and on the synchronization and desynchronization behavior of neural oscillators. Recent applications include pattern and memory association, scene analysis, and pattern recognition [10]. Chaotic oscillators have been combined with ANNs to produce Chaotic Oscillatory-based Neural Networks (CONN), which mimic neural behaviors in the human brain. One of these models is the Improved Lee Oscillator (Retrograde Signaling) model [9] which combines the original Lee Oscillator [17] with the retrograde transport mechanism in axons, known as axonal transport or axoplasmic flow [18]. Figure 1 is a graphic depiction of the Lee-oscillator (Retrograde Signaling) model.

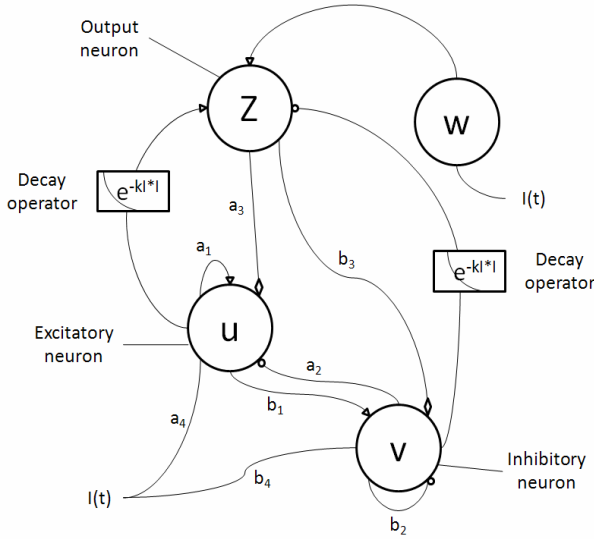


Fig 1. Lee Oscillator (Retrograde Signaling) Model [9]

As a Lee Oscillator (Retrograde Signaling) model exhibits chaotic progressive growth in its neural dynamics, it can be used as an effective chaotic bifurcation transfer unit in neural networks.

The Lee Oscillator (Retrograde Signaling) model consists

of the neural dynamics of four constitutive neural elements: u , v , w and z . The neural dynamics of each of these constituent neurons are given by

$$\begin{aligned} u(t+1) &= f[a_1 u(t) - a_2 v(t) + a_3 z(t) + a_4 I(t) - \theta_u] \end{aligned} \quad (1)$$

$$\begin{aligned} v(t+1) &= f[b_2 z(t) - b_1 u(t) - b_2 v(t) + b_4 I(t) - \theta_v] \end{aligned} \quad (2)$$

$$w(t+1) = f[I(t)] \quad (3)$$

$$z(t) = f[v(t) - u(t)]e^{-kt} + w(t) \quad (4)$$

where $u(t)$, $v(t)$, $w(t)$ and $z(t)$ are the state variables of respectively the excitatory, inhibitory, input and output neurons; $f(\cdot)$ is the hyperbolic tangent function; a_1 , a_2 , a_3 , a_4 , b_1 , b_2 , b_3 and b_4 , are the weight parameters for these constitutive neurons; θ_u and θ_v are the thresholds for excitatory and inhibitory neurons; $I(t)$ is the external input stimulus; and k is the decay constant.

III. METHODOLOGY

A. Data Preparation

The local air density, local temperature variations, local effects of cloud and rain are difficult to measure [19] and LIDAR can only measure the Doppler velocities of the wind. We make use of the Doppler velocity data derived from glide path scans of the LIDAR. The Doppler velocities data are first processed with the quality control algorithm [20]. Outliers are detected by comparing each piece of radial velocity with neighboring data points. If the difference between them is larger than a pre-defined threshold, it will be smoothed using a median-filtered value. The threshold is determined from the frequency distribution of the difference in the velocities of the adjacent range/azimuthal gates of the LIDAR over a long period of time. Data quality control is kept to a minimum in order to avoid smoothing out the genuine wind fluctuations of the atmosphere [20]. If data is missing for a particular location, any available valid velocity data from neighboring positions or timeframes is used to derive a replacement velocity value through a linear interpolation of the velocities at the neighboring points.

The training and testing data set were normalized by using minimum (-1) and maximum (+1) normalization before training and testing. Each set of training data was for the glide path at a specific time. It included the Doppler velocities on a slant range, angle of elevation, and azimuth. These were used to train the model to predict Doppler velocities along the glide path in the upcoming three minutes. The time interval between two training sets was from three to four minutes.

B. Chaotic Oscillatory Based Neural Network

The Chaotic Oscillatory Based Neural Network (CONN) is made up of a Multi-Layered Perception (MLP) Neural Network and a Lee Oscillator (Retrograde Signaling) Model with various parameter settings. The MLP neural networks constructed by one or two hidden layers with several neurons, and the activation function of the neurons in the hidden layer(s) and output layer were replaced with the Lee Oscillator (Retrograde Signaling) Model rather than with the sigmoid or hyper tangent function as in conventional neural networks.

C. Training and testing of the CONN

The CONN is trained with a month of the preprocessed Doppler velocity data, which is formatted into time intervals using a back propagation learning algorithm. A momentum term is used to speed up convergence and avoid local minima. It learns from the root mean square error between the predicted result and the measured value from the LIDAR through back propagation. In the testing process, the neural network uses the experience gained in the training process to generate the forecast for the next time interval(s).

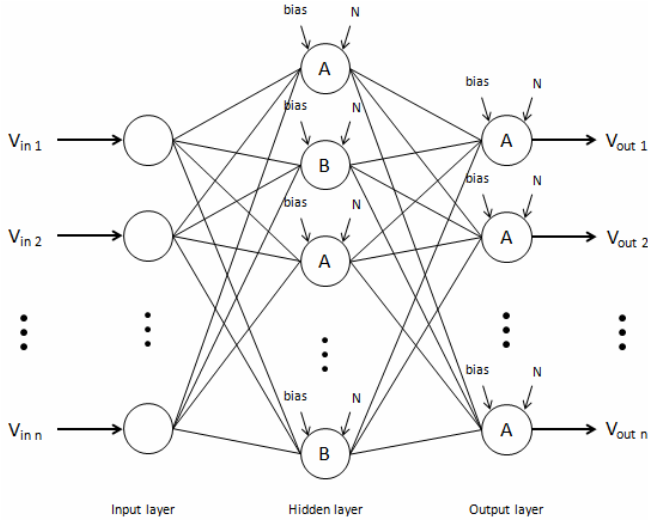


Fig 2. The structure of the CONN

Figure 2 shows the structure of the CONN used in the simulation. The current wind pattern along the selected glide path (V_{in}) which is measured by the LIDAR system will be fed into the CONN through the input nodes in the input layer. The forecast of the winds along the selected glide path (V_{out}) in the next time frame can be obtained at the output node in the output layer. Neurons in hidden layer(s) and output layer produce the output of the chaotic oscillator based on the corresponding external stimulus received from the connected neurons in the previous layer.

There can be one to two hidden layer(s) with several hidden neurons within. The number of hidden layers and hidden neurons were chosen experimentally since there is no simple clear-cut method for determining these parameters [9]. Characters A and B in the neurons indicate different parameter settings used with the Lee Oscillator (Retrograde Signaling) Model. These parameters were also chosen experimentally. Table 1 presents the values of the parameter settings that are used in the neurons, which are labeled A and B in the hidden layer(s) and output layer in Figure 2.

Parameters	Lee Oscillator (Retrograde Signaling) with Parameter sets	
	A	B
a_1	1.0	-0.7
a_2	-1.0	0.6
a_3	1.0	-0.5
a_4	-1.0	0.4
b_1	1.0	-0.7
b_2	-1.0	0.6
b_3	1.0	-0.5
b_4	-1.0	0.4
k	50.0	50.0
θ_u	0.0	0.0
θ_v	0.0	0.0

Table 1. Values of the parameter used in the CONN

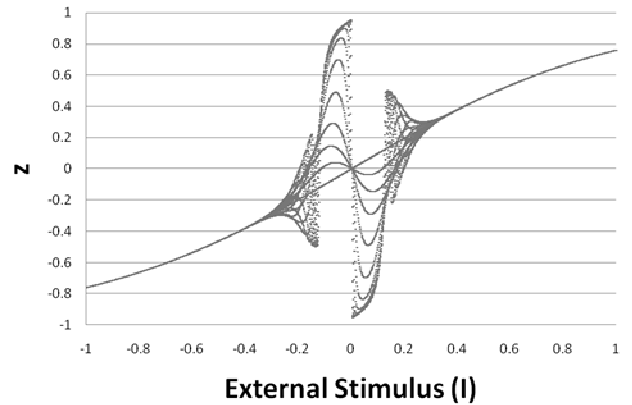


Fig 3. Bifurcation Diagram of Lee Oscillator (Retrograde Signaling) Model for Parameter set A

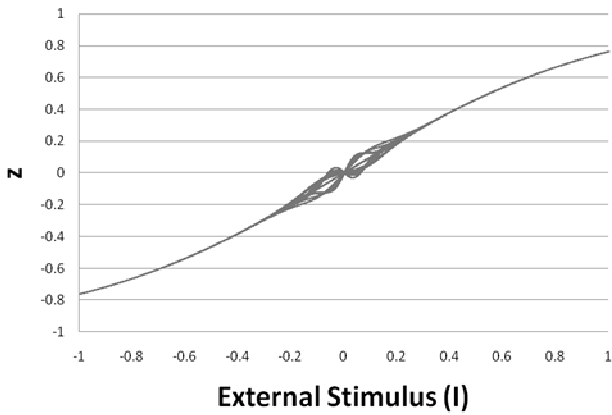


Fig 4. Bifurcation Diagram of Lee Oscillator (Retrograde Signaling) Model for Parameter set B

Figures 3 and 4 show the bifurcation diagrams of the Lee Oscillator (Retrograde Signaling) Model with parameter sets A and B. The x-axis represents the external stimulus (I) from the connected neurons in the previous layer to the chaotic oscillator. The y-axis represents the output of the chaotic oscillator corresponding to the external stimulus. The response of the Lee Oscillator (Retrograde Signaling) Model to an external input stimulus with parameter sets A and B can be categorized into two regions, the sigmoid-shape region and hysteresis region. The former denotes the non-chaotic neural activities in the oscillator. The latter denotes the chaotic behavior that results when a weak external input stimulus is received.

In [10], the parameters which used in individual neurons are predefined before the start of training process and the training process only focuses on tuning the weights among different layers of neurons. As the shape of the bifurcation is predefined, the responses of the Lee Oscillator (Retrograde Signaling) Model were limited to the outer most shell of the chaotic region.

Neural oscillators depend on parameters that have to be tuned to achieve the desired performance. However, since neural oscillators have highly nonlinear dynamics, parameters of neural oscillators are difficult to tune [21], [22]. Although there has been work on chaos control and tuning the parameters of neural oscillator, most of it concentrates on oscillation control or the frequency, amplitude and phase of the neural oscillator [21], [22], [23], and [24]. Little work has considered the shape of the bifurcation diagram used as the transfer function in CONN.

Experimental variation in the number of iterations of the same parameters set during the training process allows CONN to produce possible changes in the chaotic region of the Lee Oscillator (Retrograde Signaling) Model. Figures 5 and 6 show the appearance of the Lee Oscillator (Retrograde Signaling) Model for parameter set A at iterations 4 and 10.

The training process not only tunes the bias of neurons and the weights between input layer, hidden layer and output layer, it also adjusts the number of iterations of the Lee

Oscillator (Retrograde Signaling) Model in the output layer neurons. As the time required computing the Lee Oscillator (Retrograde Signaling) Model is directly proportional to the number of iterations that are assigned, it is also possible to improve the performance of the CONN, reducing the time required for less necessary iterations by adjusting the number of iterations used in each individual neuron during the training process.

The mechanism is that a randomly generated iteration number (N) will be assigned to each neuron in both hidden and output layers during initialization of the neural network. Neurons in the output layer will produce five different outputs by using the assigned N value. For example, if value 10 is assigned to the first neuron in the hidden layer during initialization, this neuron will produce five outputs by using $N \pm 2$ (in this example $N=8, N=9, N=10, N=11$ and $N=12$ will be used) with the same parameter set in the current epoch of training. After comparing the outputs with the actual measured data from LIDAR, the output with the smallest error value will be selected as the output of that neuron. On the other hand, the N that produces the output with the smallest error will be used to update the old N of that neuron in that training epoch and will be the initial N value of that neuron in the next epoch. Once the changes of the N value in an individual neuron become steady, the mechanism that updated the N value in that neuron will stop. We assume that the neural oscillator used in that neuron is already well trained.

By varying the N value, different possible changes in the chaotic region of the chaotic oscillator will be tested and selected heuristically in the training process. The use of the chaotic oscillator will no longer be limited to the outermost shell of the chaotic region produced by a fixed number of iterations assigned at the initialization of CONN.

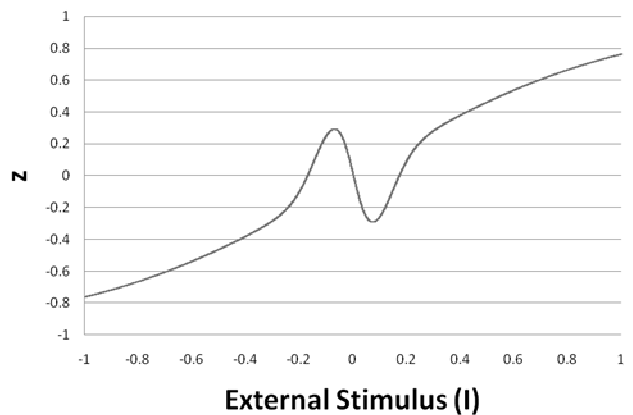


Fig 5. Lee Oscillator (Retrograde Signaling) Model for Parameter set A with iterations number 4

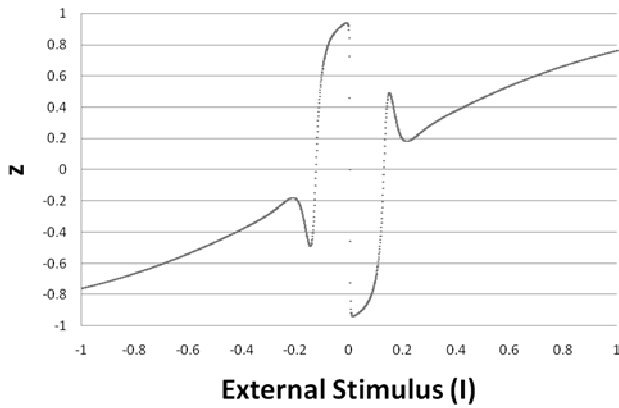


Fig 6. Lee Oscillator (Retrograde Signaling) Model for Parameter set A with iterations number 10

D. Wind shear detection in the forecast result

An algorithm called the GLide-path scan Wind shear alerts Generation Algorithm (GLYGA) has been developed by the Hong Kong Observatory to detect wind shear automatically from headwind profiles generated from LIDAR data [20]. By combining GLYGA and the forecasted results that produced by CONN, it may be possible to forecast wind shear events. We do this by first combining the forecast radial velocities along a glide path to construct a headwind profile. Differences in the velocities of adjacent data points in the headwind profile are calculated to construct a velocity increment profile. Next, the wind shear ramps are detected by comparing each data point of the profile with the neighboring points on two sides. The wind shear ramps detected from a headwind profile are prioritized using a normalized wind shear value $\Delta V/H^{1/3}$, suggested by Jones and Haynes [25], where ΔV is the total change in the headwind and H is the ramp length. If any one of the wind shear ramps exceeds 14 knots, an alert message is generated.

IV. SIMULATION

We tested the wind shear alert generation function using sea breeze data from 6 January 2009. This date was chosen because it was a day of significant wind shear with large wind shear ramps. A training set was constructed from the data recorded between 1 December 2008, 02:42:46 (UTC) and 1 January 2009, 06:03:57 (UTC) and a testing set was constructed from the data recorded between 6 January 2009, 04:03:09 (UTC) and 04:54:58 (UTC).

Figure 7 shows the overall changes of the wind along the glide path 07RA (i.e. landing at the south runway of HKIA from the west) between 6 January 2009 04:05 (UTC) and 04:56 (UTC). Figure 8 shows the forecast of the wind profile along the glide path 07RA made using the current CONN model. The x-axis shows the distance from the end of the runway in nautical miles and the y-axis shows the wind velocity in meters per second. The various gray lines indicate

the wind field along the glide path at different moments. Figure 9 provides a scatter diagram comparing the observed and the forecast headwinds between 6 January 2009 04:05 (UTC) and 04:56 (UTC). The forecasts can be seen to be fairly close to the actual observations.

Figure 10 shows headwind profiles obtained by applying the GLYGA algorithm with the actual observed LIDAR data and simulation results for the sea breeze for the period from 6 January 2009 at the arriving runway corridors 07RA with different time slots. The small figures on the left are the forecasts made by CONN. The small figures on the right are the actual observations from LIDAR. The x-axis is the distance away from the end of the runway in nautical miles. The y-axis on the left is for the head wind measured in knots. The y-axis on right hand side is the altitude of the glide path measured in feet. The detected wind shear ramp(s) are highlighted.

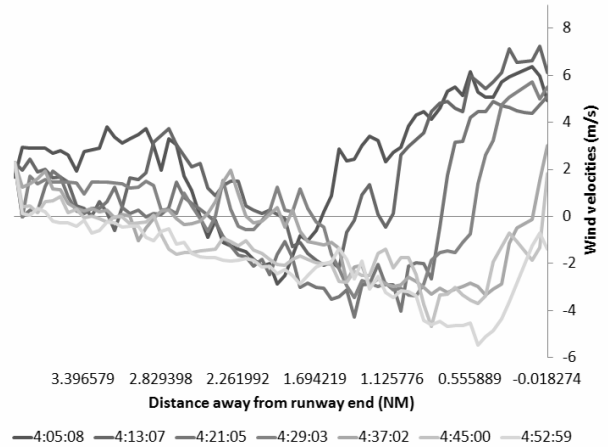


Fig 7. The observed movement of the sea breeze between 6 January 2009 04:05 and 04:56 (UTC)

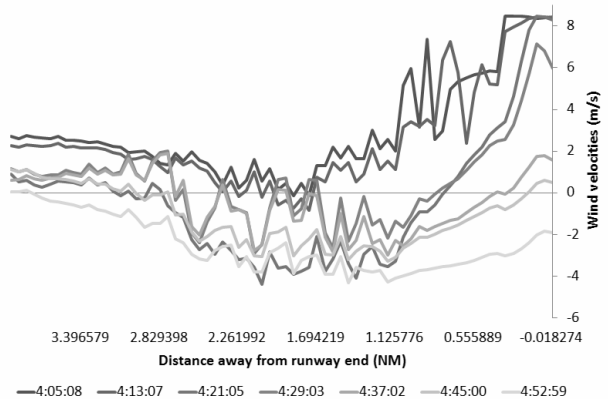


Fig 8. The forecasted radial wind velocity by CONN between 6 January 2009 04:05 and 04:56 (UTC)

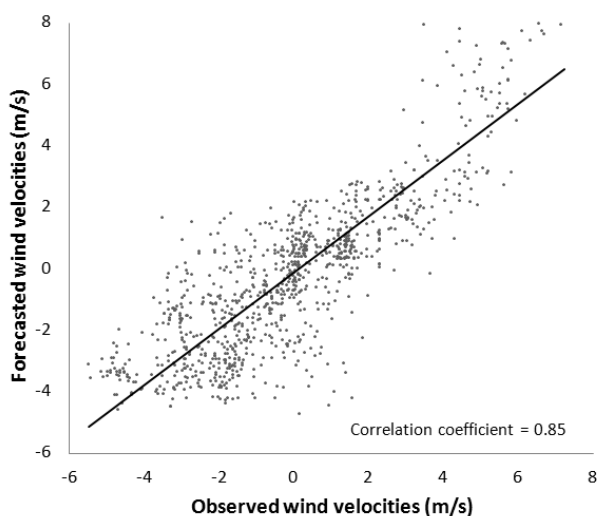


Fig 9. Forecasted versus observed headwinds

In this simulation, the forecast predicted most of the actually observed wind shear. In the period between 04:05 (UTC) and 04:56 (UTC) wind shear was successfully forecast for seven out of eight occurrences in 14 time slots. For example, one 14-knot wind shear ramp was observed between 0.3 and 1.4 NM from the end of the runway at 04:17:06 (UTC). The GLYGA algorithm captured a 15-knot wind shear ramp between 0.5 and 1.5 NM from the end of the runway at 04:17:06 (UTC). We note that the highlighted region in the forecast figures (as a predicted wind shear ramp) corresponds to the region where wind shear in fact occurred in the observed headwind profiles and they had similar size. In short, the CONN model appears to make reasonable predictions of the occurrence of the wind shear events, including the general location and magnitude of the shear.

It is fair to say that the performance of forecast drops while time is passing. Figure 11 shows the change of correlation coefficient of the forecast and actually measured data against time for a long trial. There is a sudden drop at around 180 minutes and some later fluctuation of the correlation coefficients. This sudden drop of correlation coefficient indicates the trained CONN begins to lose the skill on making valid forecast. In order to keep making valid forecast, re-training of the CONN with the last updated data will be required.

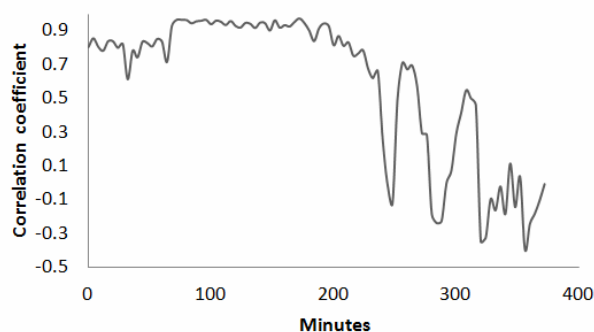


Fig 11. Correlation coefficient versus time

V. CONCLUSION

Using the LIDAR's Doppler velocity data for a meso-scale wind field, we tested CONN, a chaotic oscillatory-based neural network, for wind shear forecasting. Experimental results show that it appears to have the potential of capturing the occurrence and evolution of sudden changes in the wind along the glide paths caused by sea breeze in the vicinity of the Hong Kong International Airport. The simulation results show that Doppler velocity forecast using CONN can be transformed into headwind profile and processed with the wind shear alerting algorithm, GLYGA, that was developed by the Hong Kong Observatory. The alerts based on the CONN forecast are shown to match actual observations made using LIDAR in terms of time, location, and magnitude of the shear for a particular case of sea breeze.

In future work we will continue to focus on the winds along the glide paths and try to optimize the computational process and enhance the predictive capability of the CONN model by improving the learning algorithm and exploring new learning algorithms for both CONN and the Lee Oscillator. We will also investigate ways to automatically tune the initial parameter settings of the CONN and identify the most suitable parameter settings of the Lee Oscillator for forecasting different types of wind fluctuations. Furthermore, we will try to improve the quality of the forecasts and the alert generating results. We will do this by comparing alert messages generated from actual LIDAR data, forecasts by CONN, and actual wind shear experienced by aircraft as reported by pilots.

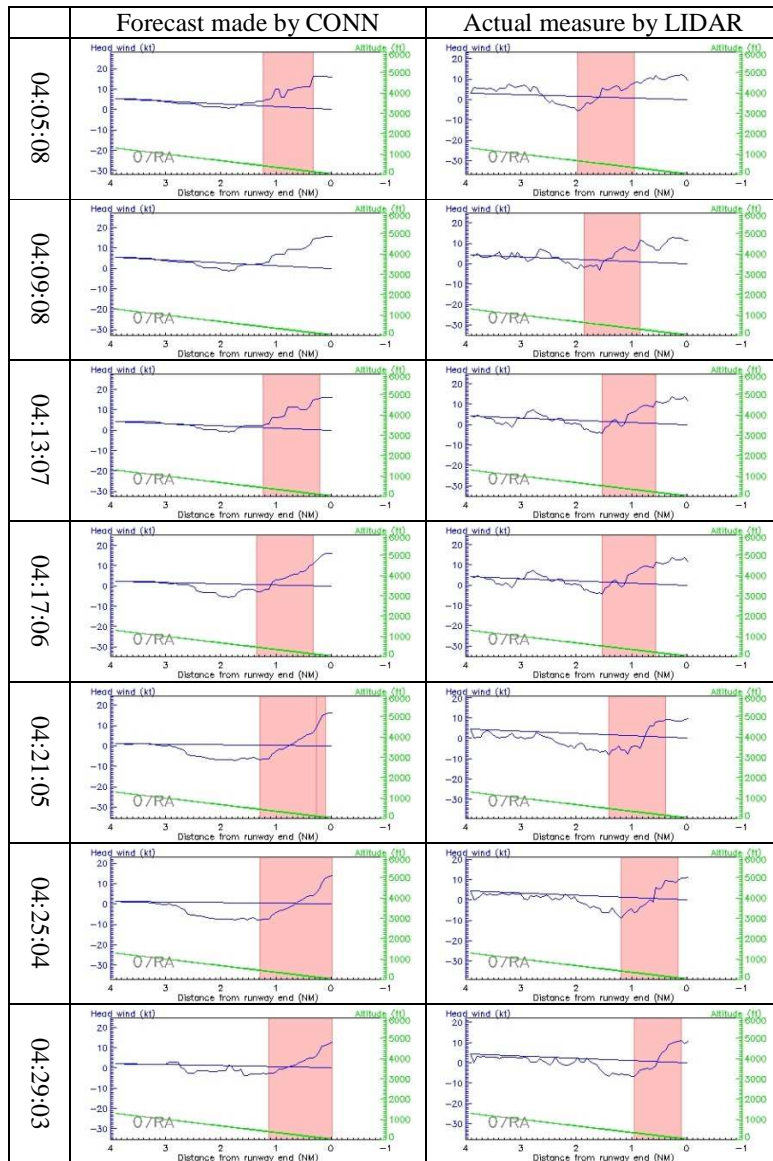
ACKNOWLEDGMENT

This work was supported in part by CERG grant B-Q05Z, and LIDAR data were kindly provided by the Hong Kong Observatory.

REFERENCES

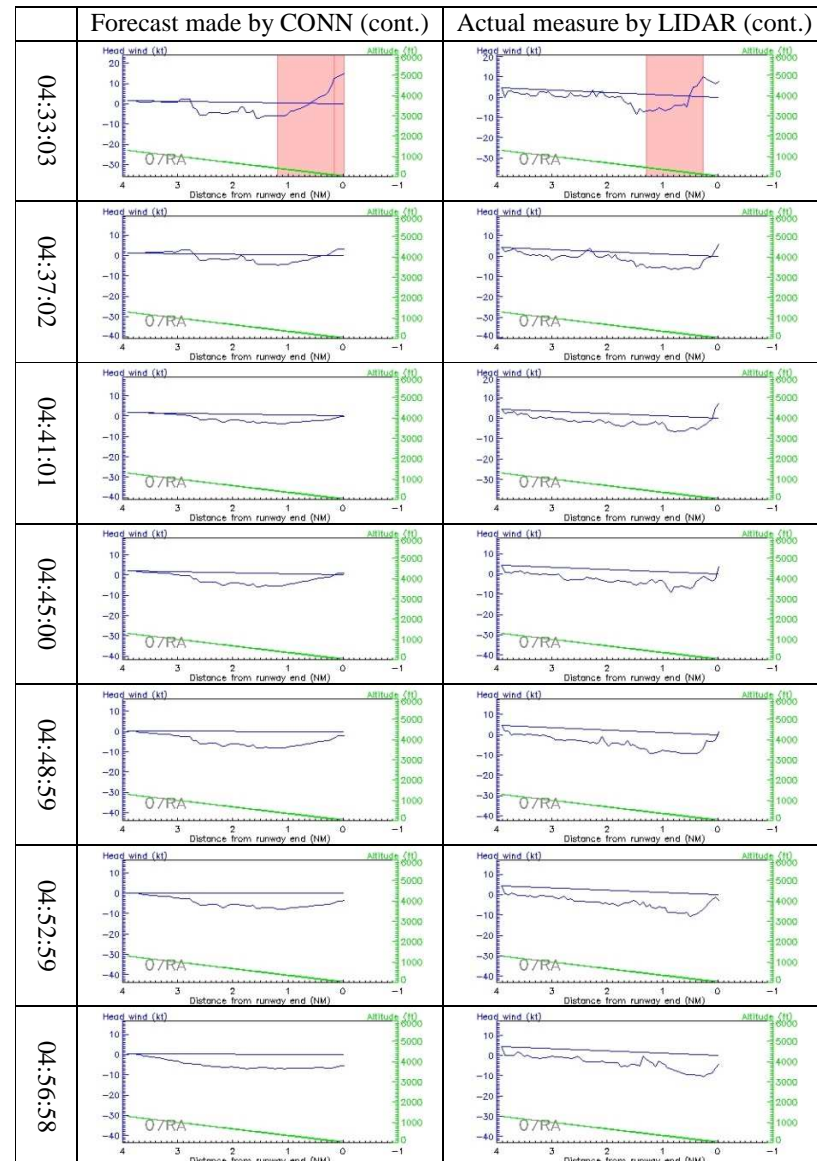
- [1] Marilyn M. Wolfson, Richard L. Delanoy, Barbara E. Forman, Robert G. Hallowell, Margita L. Pawlak, and Peter D. Smith, Automated Microburst Wind Shear Prediction, *The Lincoln Laboratory Journal*, vol. 7 (2), 1994.
- [2] Hong Kong Observatory (HKO), International Air Line Pilots' Association (IFALPA) and Guild of Air Pilots and Air Navigators

- (GAPAN), 2010: 'Wind shear and Turbulence in Hong Kong – information for pilots': <http://www.weather.gov.hk/aviat/articles/WS-turb-booklet-eng-3rd.pdf>
- [3] C.M. Shun, Hong Kong Observatory, "Wind Shear and Turbulence Alerting at Hong Kong International Airport", WMO Bulletin, vol. 53 (4), Oct. 2004.
- [4] Perez-Munuzuri, V., Souto, M.J., Casares, J. and Perez-Villar, V., "Terrain-induced focusing of wind fields in the mesoscale", Chaos, Solitons & Fractals, vol. 7 (9), pp.1479-1494, Sept. 1996.
- [5] M. Bilgili, B. Sahin, A. Yasar, "Application of artificial neural networks for the wind speed prediction of target station using reference stations data", Renewable Energy, vol. 32 (14), pp. 2350-2360, Nov. 2007.
- [6] A. More and M.C. Deo, "Forecasting wind with neural network", Marine Structures, vol. 16 (1), pp. 35-49, Jan.-Feb. 2003.
- [7] Ahmet Oztopal, "Artificial neural network approach to spatial estimation of wind velocity data", Energy Conversion and Management, vol. 47 (4), pp. 395-406, Mar. 2006.
- [8] Barbounis, T.G. Theocharis, J.B. Alexiadis, M.C. and Dokopoulos, P.S., "Long-term wind speed and power forecasting using local recurrent neural network models", IEEE Transactions on Energy Conversion, 21 (1), pp. 273-284, 2006.
- [9] M.H.Y. Wong, R.S.T. Lee and J.N.K. Liu, "Wind shear forecasting by Chaotic Oscillatory-based Neural Networks (CONN) with Lee Oscillator (Retrograde Signaling) model", In Proceedings of IEEE International Joint Conference on Neural Networks 2008 (IJCNN 2008), pp. 2040-2047, 2008.
- [10] K.M. Kwong, James N.K. Liu, P.W. Chan and Raymond S.T. Lee, "Using LIDAR Doppler Velocity Data and Chaotic Oscillatory-based Neural Network for the Forecast of Meso-scale Wind Field", IEEE World Congress on Computational Intelligence, Hong Kong, June 1-6, 2008.
- [11] Guoqiang Zhang, B. Eddy Patuwo and Michael Y. Hu, "Forecasting with artificial neural networks: The state of the art", International Journal of Forecasting, vol. 14 (1), pp. 35-62, 1 Mar. 1998.
- [12] Hisao Imai, Yuko Osana and Masafumi Hagiwara, "Chaotic Analog Associative Memory", Systems and Computers in Japan, vol. 36(4), pp. 82-90, 2005.
- [13] Xubin Zeng, Roger A. Pielke and R. Eykholt, "Chaos Theory and Its Applications to the Atmosphere", American Meteorological Society, vol. 74 (4), pp. 631-644, 1993
- [14] C.M. Shun and P.W. Chan, "Applications of an infrared Doppler LIDAR in detection of Wind shear", Journal of Atmospheric and Oceanic Technology, vol. 25, pp. 637-655, 2008.
- [15] H. R. Wilson and J. D. Cowan, "Excitatory and inhibitory interactions in localized populations," Biophys. J., vol. 12, pp. 1-24, 1972.
- [16] R.S.T. Lee, Fuzzy-neuro approach to agent applications: from the AI Perspective to Modern Ontology, Berlin Heidelberg New York Springer, 2006.
- [17] R.S.T. Lee, "A Transient-Chaotic Autoassociative Network (TCAN) Based on Lee Oscillators". IEEE Transaction on Neural Network, vol. 15 (5), pp. 1228-1243, 2004.
- [18] Irwin B. Levitan and Leonard K. Kaczmarek, The Neuron: cell and molecular biology, Oxford University Press, 2001.
- [19] Ismael Sanchez, "Short-term prediction of wind energy production", International Journal of Forecasting, vol. 22 (1), pp. 43-56, Jan.-Mar.2006.
- [20] P.W. Chan, C.M. Shun and K.C. Wu, "Operational LIDAR-based System for Automatic Wind shear Alerting at the Hong Kong International Airport", 12th Conference on Aviation, Range, & Aerospace Meteorology, American Meteorological Society, Atlanta, GA, USA, 29 Jan. - 2 Feb. 2006.
- [21] A.M. Arsenio, "Tuning of neural oscillators for the design of rhythmic motions", in Proc. IEEE Int. Conf. Robotics & Automation, San Francisco, 2000.
- [22] A.M. Arsenio, "On stability and tuning of neural oscillators: Application to rhythmic control of a humanoid robot", IEEE Int. Joint Conf. Neural Networks (IJCNN), Budapest, 2004.
- [23] Seiichi Miyakoshi, Gentaro Taga and Yasuo Kuniyoshi, "A self-tuning mechanism for the parameters of a neural oscillator", Proceedings of Robotics Symposia, Seapal Suma (Kobe), RSJ, JSME, and SICE, pp. 301-306, 2000.
- [24] Kotaro Hirasawa, Junichi Murata, Jinglu Hu, and ChunZhi Jin, "Chaos Control on Universal Learning Networks", IEEE Transactions on Systems, Man, and Cybernetics, Part C: Applications and Reviews, vol. 30 (1), pp. 95-104, Feb. 2000.
- [25] J.G. Jones and A. Haynes, "A peakspotter program applied to the analysis of increments in turbulence velocity", Royal Aircraft Establishment Tech. Rep, 1984.



(A)

(B)



(A)

(B)

Fig. 10. The headwind profiles that obtained by applying GLYGA algorithm with the forecast(A) and the actual measured LIDAR(B) data